Electronic Supplementary Information

Amino Olefin Nickel (I) and Nickel (0) Complexes as Dehydrogenation Catalysts for Amine Boranes

Matthias Vogt, Bas de Bruin, Heinz Berke, Mónica Trincado, Hansjörg Grützmacher**

[*] Dr. M. Trincado, Dipl.-Chem. M. Vogt, Prof. Dr. H. Grützmacher
Department of Chemistry and Applied Biosciences
ETH-Hönggerberg
8093 Zürich (Switzerland)
Fax: (+41) 44-633-1032
E-mail: gruetzmacher@inorg.chem.ethz.ch
Homepage: http://www.gruetzmacher.ethz.ch

Dr. Bas de Bruin
Universiteit van Amsterdam
Van 't Hoff Institute for Molecular Sciences

Prof. Dr. Heinz Berke
Universität Zürich, Anorganisch-chemisches Institut
Winterthurerstrasse 190
CH-8057 Zürich (Switzerland)

[**] This work was supported by the joint research initiative “Unconventional Approaches to the Activation of Dihydrogen (FOR 1175)” of the Swiss National Science Foundation (SNF) and the Deutsche Forschungsgesellschaft (DFG) and the ETH Zürich.

Table of Contents

A. General techniques:

Solvents were freshly distilled under argon from sodium/benzophenone (thf), from sodium/diglyme/benzphenone (*n*-hexane), or from calcium hydride (CH_2Cl_2). Unless otherwise stated all manipulations were performed under inert argon atmosphere. Air-sensitive compounds were stored and weighed in a glovebox (Braun MB 150 B-G system), and reactions on small scales were performed directly in the glovebox. Solution NMR spectra were recorded on Bruker Avance 700, 300, 250 spectrometers. The chemical shifts (δ) are measured according to IUPAC[1] and expressed in ppm relative to TMS, Et_2O-BF_3 and H_3PO_4 for ^{1}H, ^{11}B, ^{13}C, and ^{31}P respectively. Coupling constants *J* are given in Hertz [Hz] as absolute values. The multiplicity of the signals is indicated as s, d, t, or m for singlets, doublets, triplets, or multiplets, respectively. The abbreviation br. is given for broadened signals. Quaternary carbon atoms are indicated as C_{quart}, aromatic units as CH_{ar} and CH_{ar} when not noted otherwise. The olefinic protons and ^{13}C atoms of the $C{=}C_{trop}$ unit in the central seven-membered ring are indicated as CH_{olefin} and CH_{olefin}, respectively. IR spectra were measured on a Perkin–Elmer 2000 FT-IR spectrometer with a KBr beamsplitter. UV/vis spectra were recorded on a UV/vis/NIR lambda 19 spectrometer in 5 mm quartz cuvettes (200-1000 nm). Mass spectra were recorded on BRUKER Daltronics maXis (ESI, UHR-TOF), BRUKER Daltronics Ulta Flex II (MALDI, TOF) and VARIAN IonSpec (MALDI-FT-ICR) of the ETH Zurich LOC MS Service facility. Magnetic measurements were performed on a SQUID (Superconducting Quantum Interference Device) Magnetometer MPMS 5S of 'Quantum Design Inc.' in a temperature range of 2-300 K at a field of 1000 Oe. The effective magnetic moment μ_{eff} was calculated in the temperature range of 18-260 K for **2**. EPR measurements were performed on a BRUKER EMX 080 equipped with a microwave-bridge ER 041 XG and a dielectric mixing resonator ER 4117 D-MVT.

B. Syntheses and Physical data

[(Ni(OOCCF$_3$)$_2$)] 1: [Ni(CO_3)] (2.00 g, 17 mmol, 1 eq.), was put in a 250 mL Schlenk flask equipped with a reflux condenser and suspended in trifluoroacetic anhydride (11.7 mL, 84 mmol, 5 eq). To the vigorously stirred greenish mixture trifluoroacetic acid (1.6 mL, 20 mmol, 1.2 eq) was added and heated at reflux at 80 °C under evolution of CO_2 gas for 1 h. Subsequently, 20 mL of trifluoroacetic acid and 10 mL trifluoroacetic anhydride were added and the reaction mixture was refluxed for 18 h under evolution of CO_2 gas affording a homogenous green solution. After cooling to room temperature, the condenser was exchanged for a distillation bridge and the excess of the anhydride and trifluoro acetic acid was removed by distillation. The obtained green solid was dried at 100°C in high vacuum for 72 h. A significant color change of the solid to pale green was observed. Complete removal of the trifluoro acetic acid was confirmed by pH indication of an aqueous solution of a small sample of the pale green product. Quantitative yield. UV/VIS (THF*):* λ_{max} = 410 nm (shoulder), 600-700 nm (br shoulder). IR: $\tilde{\nu}$ (cm^{-1}) = 1682 s, 1463 w, 1188 s, 1140 s, 1028 m, 919 w, 876 m, 850 m, 794 s, 726 s. MP > 230 °C.

[Ni(trop$_2$NH)(OOCCF$_3$)] 2 : A 20 mL Schlenk tube was charged with (trop$_2$NH) (200 mg, 0.50 mmol, 1 equiv). The solid was suspended in 3 mL THF and [Ni($OOCCF_3$)$_2$] **1** (142 mg, 0.50 mmol, 1 equiv) was subsequently added. An excess of zinc powder (327 mg, 5.00 mmol, 10 equiv) was added to the pale greenish solution. The mixture was allowed to stir over night before the zinc powder was

filtered off the dark green solution. Subsequently, 2 mL $^{i}Pr_2O$ was added to the filtrate and the mixture was layered with 3 mL of *n*-hexane. Large deep green needles formed within 24 h at room temperature (also suitable for single crystal X-ray diffraction analysis). The supernatant solution was decanted, the obtained crystals were washed with three portions of 1 mL cold $^{i}Pr_2O$, and finally dried in a stream of argon. Yield 202 mg, 71%. UV/VIS (THF) λ_{max}: 252 nm, br 533-329 nm peak at 350 nm. IR: $\tilde{\nu}$ (cm^{-1}) = 3245 w, 3050-2846 w, 1635 s, 1487 m, 1205 m, 1182 s, 1135 s, 987 m, 843 m, 761 w, 739 m, 725 m, 659 w. MS (ESI TOF m/z) $[Ni(trop_2NH)]^+$ 455.1158 found, 455.1178 calc (error -4.4 ppm). MP > 220 °C. μ_{eff} = 1.81 μ_B. MP > 220 °C.

[Ni(trop$_2$NH)(PPh$_3$)] 3 : A 10 mL Schlenk tube was charged with $trop_2NH$ (200 mg, 0.50 mmol, 1 equiv). The solid was dissolved in 3 mL DME. Subsequently $[Ni(OOCCF_3)_2]$ (142 mg, 0.50 mmol, 1 equiv) and PPh_3 (131 mg, 0.50 mmol, 1 equiv) were added. To the pale greenish solution, an excess of zinc powder (327 mg, 5.00 mmol, 10 eq) was added and the mixture was allowed to stir for 48 h. From the dark red solution the excess zinc powder was filtered off through a plug of Celite and the filtrate was diluted with 2 mL of $^{i}Pr_2O$ and layered with 3 mL *n*-hexane. After approximately 3 h hours, large deep red crystals (also suitable for single crystal x-ray analysis) start to precipitate. The mother liquor was decanted, the obtained crystals were washed with $^{i}Pr_2O$ (3x 2.5 mL) and subsequently dried in a stream of argon. The mother liquor was layered with *n*-hexane and a second fraction of the red crystalline product was obtained following the procedure described above. Overall yield 80 % 257 mg. The *n*-hexane layered solution can also be seeded with previous obtained crystals of **3**, in this way the crystallization process can be accelerated. ^{1}H NMR (300 MHz, [D$_8$]-THF) d ppm 1.09 (br, s, 1 H, N*H*) 4.35 (s, 2 H, CH_{benzyl}) 4.39 (dd, $^3J_{HH}$ = 9.80 Hz, $^3J_{PH}$ =14.30 Hz, 2 H, CH_{olefin}) 5.12 (dd, $^3J_{HH}$ = 9.87 Hz, $^3J_{PH}$ =3.18 Hz, 2 H, , CH_{olefin}) 6.13 (d, $^3J_{HH}$ = 7.58 Hz, 2 H, CH_{ar}) 6.52 (dd, $^3J_{HH}$ = 5.14, $^3J_{HH}$ = 3.67 Hz, 2 H, CH_{ar}) 6.68 (m, 6 H, CH_{ar}) 6.88 (m, 6 H, CH_{ar}) 7.20 (m, 15 H, CH_{ar}). ^{13}C{^{1}H}-NMR (75 MHz, [D$_8$]-THF) d ppm 67.9 (d, $^2J_{PC}$ = 7.9 Hz, 2 C, CH_{olefin}) 69.5 (s, 2 C, CH_{olefin}) 70.4 (s, 2 C, CH_{benzyl}) 122.9 (d, $^4J_{PC}$ = 1.5 Hz, 2 C, CH_{ar}) 123.9 (s, 2 C, CH_{ar}) 126.6 (s, 2 C, CH_{ar}) 126.8 (s, 2 C, CH_{ar}) 127.1 (s, 2 C, CH_{ar}) 127.6 (s, 2 C, CH_{ar}) 127.8 (m, 9 C, C$H_{ar\text{-}Ph3}$) 128.7 (d, $^4J_{PC}$ = 2.7 Hz, 2 C, CH_{ar}) 129.0 (d, $^5J_{PC}$ = 1.5 Hz, 2 C, CH_{ar}) 132.4 (d, $^2J_{PC}$ = 11.6 Hz, 6 C, C$H_{ar\text{-}PPh3}$) 133.8 (d, $^5J_{PC}$ =1.5 Hz, 2 C, CH_{ar}) 135.0 (d, $^1J_{PC}$ = 29.5 Hz, 3 C, $C_{quart\text{-}PPh3}$) 138.0 (d, $^3J_{PC}$ = 2.7 Hz, 2 C, C_{quart}) 138.9 (s, 2 C, C_{quart}) 139.7 (d, $^3J_{PC}$ = 1.8 Hz, 2 C, C_{quart}). ^{31}P{^{1}H}-NMR (101.3 MHz; [D$_8$]-THF): δ (ppm) = 39.8 s, 1P, PPh_3. UV/VIS (THF): λ_{max} = 252 nm, 329 nm (shoulder). IR: $\tilde{\nu}$ (cm^{-1}) = 3050–3002 w, 2852 w, 1684 s, 1597 m, 1470 s, 1430 s, 1408 w, 1307 w, 1208 s, 1154 s, 1088 s, 1056 w, 1027 w, 998 m, 973 w, 941 w, 924 w, 900 w, 850 m, 798 m, 759 w, 741 s, 733 s, 640 s, 650 w, 638 w. MS (MALDI FT-ICR 3-HPA, m/z) [Nitrop$_2$NH$^+$] 455.1192 (found), 455.1179 (calc) (error +2.86 ppm). M.P. 210-213 °C decomp.

C. Experimental protocols for the formation of hydride complexes 8 and 9.

a) To a solution of dimethylamine borane **4** (1.2 mg, 0.020 mmol, 1 equiv) and *t*BuOK (2.2 mg, 0.020 mmol, 1 equiv) in [D_8]-THF (0.5 mL) in a *J.Young* NMR tube was added a solution of [Ni(trop$_2$NH)(OOCCF$_3$)] **2** (11.0 mg, 0.020 mmol, 1 equiv) in [D_8]-THF (0.2 mL). The reaction resulted in the formation of the hydride bridged complex **8** and a small concentration of the mononuclear nickel hydride **9** (Figure 1).
b) To the reaction mixture from a) was added an additional equivalent of *t*BuOK (2.2 mg, 0.020 mmol) in [D_8]-THF (0.1 mL). Initial formation of complex **9** is observed.
c) To a solution of dimethylamine borane (3.5 mg, 0.060 mmol, 3 equiv) and *t*BuOK (6.7 mg, 0.060 mmol, 3 equiv) in [D_8]-THF (0.5 mL) in a *J.Young* NMR tube was added a solution of [Ni(trop$_2$NH)(OOCCF$_3$)] **2** (11.0 mg, 0.020 mmol, 1 equiv) in [D_8]-THF (0.2 mL).
d) The highest relative presence of complex **9** was observed in the analysis of the reaction mixture from d) after 30 min (Figure 1).

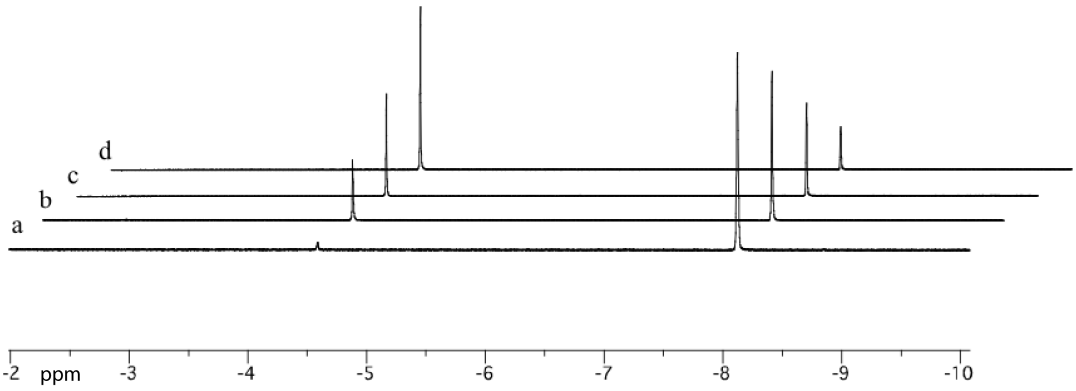

Figure 1. Sections (hydride area) of the *in situ* recorded ^{1}H NMR (700.13 MHz, 298 K) spectra of complexes **8** (s -8.12 ppm) and **9** (s -4.59 ppm) from the reactions in [D8]-THF: a) **4** (1 eq), *t*BuOK (1 eq) and **2** (1 eq); b) **4** (1 eq), *t*BuOK (2 eq) and **2** (1 eq). c) **4** (3 eq), *t*BuOK (3 eq) and **2** (1 eq) after 5 min. d) Evolution of c) after 30 min.

e) To a solution of dimethylamine borane **4** (1.2 mg, 0.020 mmol, 1 equiv) and K[Me_2NBH_3] (5.8 mg, 0.060 mmol, 3 equiv)[3] in [D_8]-THF (0.5 mL) in a *J.Young* NMR tube was added a solution of [Ni(trop$_2$NH)(OOCCF$_3$)] **2** (11 mg, 0.020 mmol, 1 equiv) in [D_8]-THF (0.2 mL). The reaction resulted in the exclusive formation of the hydride bridged complex **8.**
f) To the reaction mixture e) was added *t*BuOH (4.4 mg, 0.060 mmol, 3 equiv), evolution of H_2 and initial formation of complex **9** is observed.
Complexes **8** and **9** are relatively stable in solution for at least 24 h without apparent decomposition. The hydride-bridging coordination mode and the *trans* disposition of both trop ligands in **8** have been unambiguously demonstrated by 1D and 2D-NMR experiments (see Figure 2).

[K][(Ni(trop$_2$NH))$_2$H] 8:

The proton resonance of the NH moiety was identified by two-dimensional NMR experiments: (HH-COSY gave cross-peaks for the NH ^{1}H NMR resonance with both ^{1}H NMR resonances of the C$H_{benzylic}$ protons ($^3J_{HH}$), see Figure 2 below; CH-HMQC gave cross peaks of the NH proton resonance with the ^{13}C NMR resonances of the benzylic carbon atoms $C_{benzylic}$ (71.5 ppm and 71.6 ppm; $^2J_{HC}$); Accordingly, the CH-HMBC NMR spectrum shows cross peaks to the ^{13}C NMR resonances of the quaternary carbon atoms C_{quart} of the benz-anelated rings of the trop backbone (133.4 ppm and 134.0 ppm ppm; $^3J_{HC}$).

^{1}H NMR (700.13 MHz, [D$_8$]-THF) δ ppm -8.12 (s, 1 H, Ni$H_{hydride}$) 1.89 (br, s, 2 H, NH) 2.72 (d, $^3J_{HH}$ = 14 Hz, 2 H, CH_{olefin}) 4.19 (s, 2 H, CH_{benzyl}) 4.33 (s, 2 H, CH_{benzyl}) 4.34 (d, $^3J_{HH}$ = 7 Hz, 2 H, CH_{olefin}) 4.39 (d, $^3J_{HH}$ = 14 Hz, 2 H, CH_{olefin}) 4.59 (d, $^3J_{HH}$ = 7 Hz, 2 H, CH_{olefin}) 6.06 (d $^3J_{HH}$ = 7 Hz, 2 H, CH_{ar}) 6.32 (t $^3J_{HH}$ = 7 Hz, 2 H, CH_{ar}) 6.41-6.52 (m, 8 H, CH_{ar}) 6.62 (m, 2 H, CH_{ar}) 6.71 (d $^3J_{HH}$ = 7 Hz, 2 H, CH_{ar}) 6.77 (d $^3J_{HH}$ = 7 Hz, 2 H, CH_{ar}) 6.92 (d $^3J_{HH}$ = 7 Hz, 2 H, CH_{ar}) 7.00 (d $^3J_{HH}$ = 7 Hz, 2 H, CH_{ar}).^{13}C{^{1}H} NMR (176.1 MHz, [D$_8$]-THF) δ ppm 55.8 (s, 2 C, CH$_{olefin}$) 55.9 (s, 2 C, CH$_{olefin}$) 59.4 (s, 2 C, CH$_{olefin}$) 62.4 (s, 2 C, CH$_{olefin}$) 71.5 (s, 2 C, CH$_{benzyl}$) 71.6 (s, 2 C, CH$_{benzyl}$) 119.2 (s, 2 C, CH$_{ar}$) 119.6 (s, 2 C, CH$_{ar}$) 120.5 (s, 2 C, CH$_{ar}$) 121.0 (s, 2 C, CH$_{ar}$) 125.7 (s, 2 C, CH$_{ar}$) 126.2 (s, 2 C, CH$_{ar}$) 126.4 (s, 2 C, CH$_{ar}$) 126.5 (s, 2 C, CH$_{ar}$) 126.6 (s, 2 C, CH$_{ar}$) 127.4 (s, 2 C, CH$_{ar}$) 127.6 (s, 2 C, CH$_{ar}$) 128.0 (s, 2 C, CH$_{ar}$) 128.8 (s, 2 C, CH$_{ar}$) 129.2 (s, 2 C, CH$_{ar}$) 129.6 (s, 2 C, CH$_{ar}$) 130.2 (s, 2 C, CH$_{ar}$) 133.4 (s, 2 C, C_{quart}) 134.0 (s, 2 C, C_{quart}) 137.4 (s, 2 C, C_{quart}) 138.3 (s, 2 C, C_{quart}) 141.2 (s, 2 C, C_{quart}) 142.7 (s, 2 C, C_{quart}) 145.1 (s, 2 C, C_{quart}) 146.8 (s, 2 C, C_{quart}).

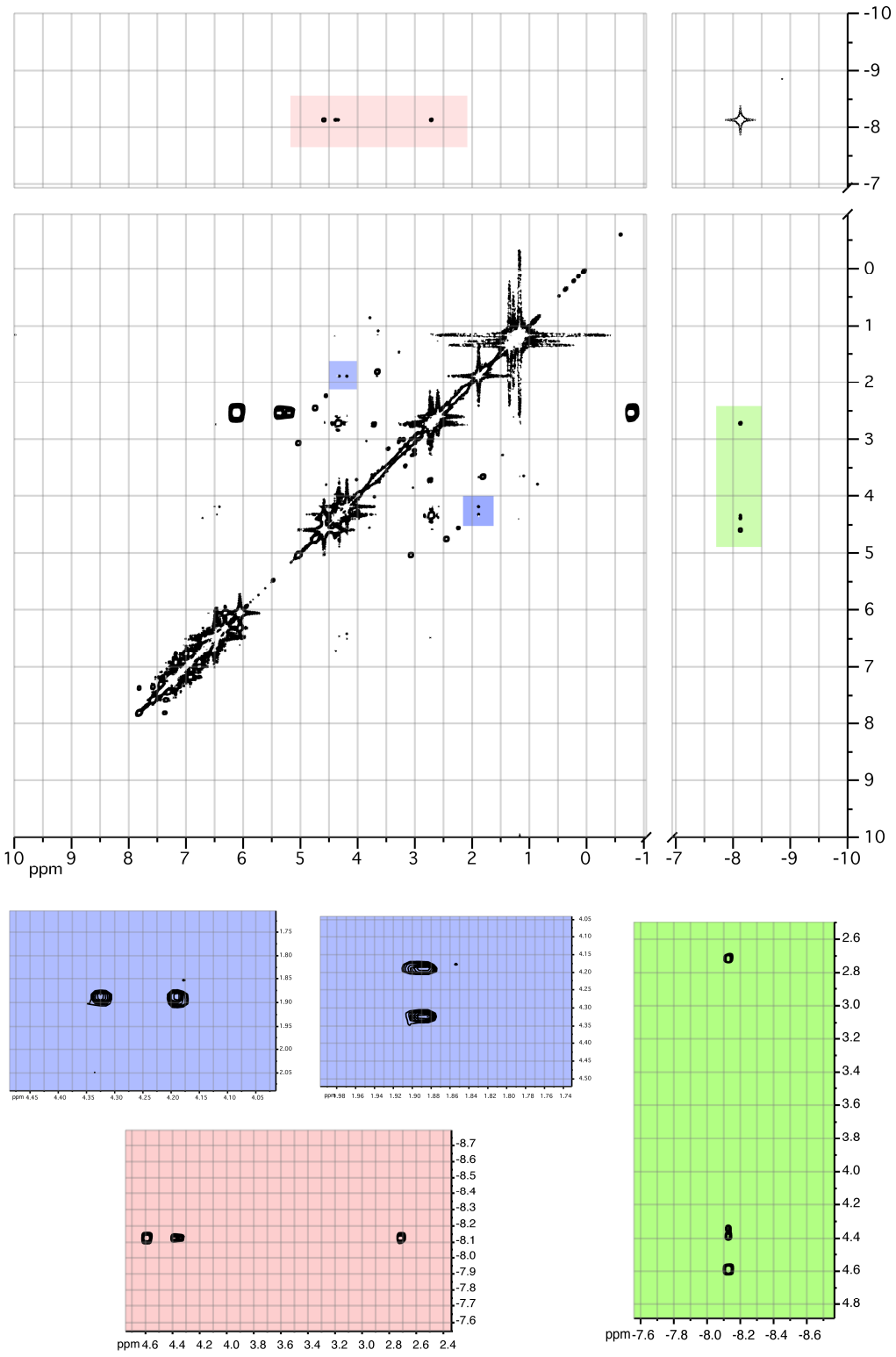

Figure 2. HH-COSY spectrum of **[K][(Ni(trop$_2$NH))$_2$H] 8,** 700.13 MHz, [D$_8$]-THF. Cross-peaks of the bridging hydride resonance (-8.12 ppm, s) and the olefinic resonances centered at 2.72 ppm (d, $^3J_{HH}$ = 14 Hz), 4.34 ppm (d, $^3J_{HH}$ = 7 Hz), 4.39 ppm (d, $^3J_{HH}$ = 14 Hz) and 4.59 ppm (d, $^3J_{HH}$ = 7 Hz) respectively, are shown magnified in separate parts of the spectra (red and green box). Cross-peaks ($^3J_{HH}$) for the NH resonance (s, 1.89 ppm) and both resonances of the C$H_{benzylic}$ protons (s 4.18 and s 4.33 ppm) are marked in blue.

[K][Ni(trop$_2$NH)H] 9:
^{1}H NMR (700.13 MHz, [D$_8$]-THF) δ ppm -4.59 (s, 1 H, Ni*H*$_{hydride}$) 1.41 (s, br, 1 H, N*H*) 4.00 (d, $^3J_{HH}$ = 9 Hz, $^3J_{HH}$ = 7 Hz 2 H, C*H*$_{olefin}$) 4.20 (s, 2 H, C*H*$_{benzyl}$) 4.28 (dd, $^3J_{HH}$ = 9 Hz, $^3J_{HH}$ = 3 Hz, 2 H, C*H*$_{olefin}$) 6.43 (m, 2 H, C*H*$_{ar}$) 6.49 (m, 4 H, C*H*$_{ar}$) 6.56 (m, 2 H, C*H*$_{ar}$) 6.70 (dt, J_{HH} = 8 Hz, J_{HH} = 1 Hz 2 H, C*H*$_{ar}$) 6.83 (br d, J_{HH} = 7 Hz, 2 H, C*H*$_{ar}$) 6.86 (dt, J_{HH} = 8 Hz, J_{HH} = 1 Hz 2 H, C*H*$_{ar}$) 7.21 (br d, J_{HH} = 7 Hz, 2 H, C*H*$_{ar}$). ^{13}C{^{1}H}-NMR (176.1 MHz, [D$_8$]-THF) δ ppm 52.7 (s, 2 C, *C*H$_{olefin}$) 55.3 (s, 2 C, *C*H$_{olefin}$) 70.9 (s, 2 C, *C*H$_{benzyl}$) 119.0 (s, 2 C, *C*H$_{ar}$) 120.7 (s, 2 C, *C*H$_{ar}$) 126.0 (s, 2 C, *C*H$_{ar}$) 126.4 (s, 2 C, *C*H$_{ar}$) 126.7 (s, 2 C, *C*H$_{ar}$) 127.4 (s, 2 C, *C*H$_{ar}$) 129.1 (s, 2 C, *C*H$_{ar}$) 129.9 (s, 2 C, *C*H$_{ar}$) 133.0 (s, 2 C, *C*$_{quart}$) 139.6 (s, 2 C, *C*$_{quart}$) 142.0 (s, 2 C, *C*$_{quart}$) 147.8 (s, 2 C, *C*$_{quart}$).

D. **Dehydrogenation of Me$_2$HN-BH$_3$ 4 catalyzed by [Ni(trop$_2$NH)(OOCCF$_3$)] 2**. In a typical experiment, to a solution of dimethylamine borane **4** (59.0 mg, 1 mmol) in THF (1 mL) was added *t*BuOK (3.4 mg, 0.03 mmol) or K[Me$_2$NBH$_3$] (2.9 mg, 0.03 mmol). [Ni(trop$_2$NH)(OOCCF$_3$)] **2** (5.7 mg, 0.01 mmol) was immediately added, vigorous evolution of hydrogen gas and formation of a brownish solution was observed. The reaction mixture was analyzed by ^{1}H and ^{11}B NMR spectroscopy, confirming that the product obtained is the cyclic dimer (NMe$_2$BH$_2$)$_2$ **6**.Addition of diethyl ether to the mixture precipitated the nickel salts and allowed their facile filtration from the solution. Subsequently, the solvent was removed in *vacuo* and the obtained colorless solid was sublimed on a steam bath using a cooling finger under argon atmosphere. The spectroscopic data was compared with previously reported.[4]
^{1}H NMR (300 MHz, C$_6$D$_6$): δ = 3.0–1.9 (q, br, $^1J_{BH}$ = 114 Hz, B*H$_2$*), 2.44 (s, C*H$_3$*); ^{13}C {^{1}H} NMR (75 MHz, C$_6$D$_6$): δ = 52.3 ppm; ^{11}B NMR (96.3 MHz, C$_6$D$_6$): δ = 5.10 (t, $^1J_{BH}$ = 112 Hz, *B*H$_2$).
ATR IR (ν in cm^{-1}) 3018 m, 2960 s, 2860 m, 2810 m, 2440 s, 2370 s, 2230 m, 1470 m, 1240 s, 1193 s, 1150 s, 1048 m, 965 s, 812 m.

The same protocol was followed with complex [Ni(trop$_2$NH)PPh$_3$] **3** (7.2 mg, 0.01 mmol). During the monitoring of the reaction with the complex **3**, formation of the linear dimer NMe$_2$HBH$_2$NMe$_2$BH$_3$ **7** was observed. This compound was isolated by addition of diethyl ether, filtration and subsequent evaporation of the solvent under *vacuo*. Recrystallization of the residue from diethyl ether/*n*-hexane ether afforded the product as a colorless solid. The obtained spectroscopic data is in good agreement with with data previously reported.[5]
M.P. > 230 ˚C
^{1}H NMR (300 MHz, C$_6$D$_6$): δ = 5.05 (s, br, 1H, N*H*), 2.03 (t, br, $^1J_{BH}$ = 110 Hz, 2H, B*H$_2$*), 1.85 (q, br, $^1J_{BH}$ = 96 Hz, 3H, B*H$_3$*), 2.45 (s, 6H, C*H$_3$*), 1.92 (s, 3H, C*H$_3$*) 1.89 (s, 3H, C*H$_3$*) ppm; ^{13}C {^{1}H} NMR (75 MHz, C$_6$D$_6$): δ = 52.6, 42.8 ppm; ^{11}B NMR (96.3 MHz, C$_6$D$_6$): δ = 2.27 (t, $^1J_{BH}$ = 109 Hz, *B*H$_2$), -12.69 (q, $^1J_{BH}$ = 94 Hz, *B*H$_3$) ppm.
ATR IR (ν in cm^{-1}) 3020 m, 2447 s, 2390 s, 2340 s, 2345 s, 2313 s, 2287 s, 2295 s, 2165 m, 2109 m, 2058 m, 1420 m, 1115 m, 850 m.

E. Volumetric measurement of hydrogen

In a typical experiment, dimethylamine borane **4** (59 mg, 1 mmol) and *t*BuOK (3.4 mg, 0.03 mmol) were dissolved in THF (0.5 mL) in a 25 mL 2-neck round bottom flask under inert atmosphere. The flask was closed with a tight-fitting rubber septum. A solution of catalysts **2** (5.6 mg, 0.01 mmol) in THF (0.5 mL) was added via syringe to the stirred amine borane solution. For the reaction of **2** (1.9 mg, 0.003 mmol), *t*BuOK (1.1 mg, 0.01 mmol) was employed; for the reaction with **B** (1.5 mg, 0.002 mmol) and 0.006 mmol of *t*BuOK.
Timing and measurement were started when the catalyst was injected into the amine borane solution. The hydrogen gas was collected in a water-filled, pressure equalized gas-burette connected to the 2nd neck of the flask via a rubber tube. The volume of hydrogen gas collected was recorded periodically until the reaction was complete.

F. Details of the structure determinations of 2 and 3.

Crystals of **2** and **3** were obtained as described in Part B.
The crystals were measured on a 'BRUKER APEX' platform diffractometer with CCD area detector; $Mo_{K\alpha}$ radiation (0.71073 Å). The refinement against full matrix (versus F^2) was done with SHELXTL (ver. 6.12) and SHELXL-97. Empirical absorption correction was done with SADABS (ver. 2.03). All non-hydrogen atoms were refined anisotropically. The contribution of the hydrogen atoms, in their calculated positions, was included in the refinement using a riding model. For details see the crystallographic table for each compound below.
Supplementary crystallographic data for the reported structures is available using the CCDC identification codes given in the tables below. These data can be obtained free of charge via www.ccdc.cam.ac.uk/conts/retrieving.html (or from the Cambridge Crystallographic Data Centre, 12 Union Road, Cambridge CB21EZ, UK; fax:

Table 1. Crystal data and structure refinement for [Ni(trop$_2$NH)(OOCCF$_3$)]x(THF) **2**.

Identification code	CCDC 767256	
Empirical formula	$C_{32}H_{23}F_3N_1Ni_1O_2$ ($C_4H_8O_1$)	
Formula weight	641.33	
Temperature	200(2) K	
Wavelength	0.71073 Å	
Crystal system	Monoclinic	
Space group	P 21/n	
Unit cell dimensions	a = 13.992(3) Å	a= 90 °.
	b = 11.424(2) Å	b= 101.06(3) °.
	c = 18.291(4) Å	g = 90 °.
Volume	2869.5(10) Å^3	
Z	4	
Density (calculated)	1.485 Mg/m^3	
Absorption coefficient	0.735 mm^{-1}	
F(000)	1332	
Crystal size	0.20 x 0.15 x 0.11 mm^3	
Theta range for data collection	2.03 ° to 28.30 °.	
Index ranges	-18<=h<=18, -15<=k<=15, -24<=l<=24	
Reflections collected	29172	
Independent reflections	7123 [R(int) = 0.0388]	
Completeness to theta = 28.30 °	99.7 %	
Absorption correction	Empirical	
Max. and min. transmission	0.9235 and 0.8669	
Refinement method	Full-matrix least-squares on F^2	
Data / restraints / parameters	7123 / 0 / 521	
Goodness-of-fit on F^2	1.029	
Final R indices [I>2sigma(I)]	R1 = 0.0405, wR2 = 0.0957	
R indices (all data)	R1 = 0.0495, wR2 = 0.1010	
Largest diff. peak and hole	0.692 and -0.237 e.Å^{-3}	

Table 2. Crystal data and structure refinement for [Ni(trop$_2$NH)(PPh$_3$)] **3**.

Identification code	CCDC 767257
Empirical formula	$C_{48}H_{38}N_1Ni_1P_1$
Formula weight	718.47
Temperature	100(2) K
Wavelength	0.71073 Å
Crystal system	Triclinic
Space group	P -1
Unit cell dimensions	a = 11.4130(11) Å a= 98.677(2) °.
	b = 12.0679(11) Å b= 95.682(2) °.
	c = 14.4208(13) Å g = 114.432(2) °.
Volume	1758.7(3) Å^3
Z	2
Density (calculated)	1.357 Mg/m^3
Absorption coefficient	0.634 mm^{-1}
F(000)	752
Crystal size	0.25 x 0.20 x 0.16 mm^3
Theta range for data collection	1.45 ° to 28.33 °.
Index ranges	-15<=h<=15, -16<=k<=16, -19<=l<=19
Reflections collected	18304
Independent reflections	8645 [R(int) = 0.0340]
Completeness to theta = 28.33 °	98.7 %
Absorption correction	Empirical
Max. and min. transmission	0.9054 and 0.8576
Refinement method	Full-matrix least-squares on F^2
Data / restraints / parameters	8645 / 0 / 463
Goodness-of-fit on F^2	1.037
Final R indices [I>2sigma(I)]	R1 = 0.0434, wR2 = 0.1099
R indices (all data)	R1 = 0.0530, wR2 = 0.1157
Largest diff. peak and hole	1.198 and -0.397 e. Å^{-3}

G. DFT geometry optimizations, EPR property calculations, experimental EPR measurements and spectral simulations.

DFT:

DFT geometry optimizations were carried out with the Turbomole program[6a] coupled to the PQS Baker optimizer.[7] Geometries were optimized at the BP86[6] level using the Turbomole SV(P) basisset[6c,d] on all atoms.

EPR parameters[9] were calculated with the Orca[10] program system using the hybrid PBE0[11] functional and the TZVP basis set[6d], as well as with the ADF[12] program system using the BP86[8] functional with the ZORA/TZP basis sets supplied with the program (all electron, core double zeta, valence triple zeta polarized basis set on all atoms), each using the coordinates from the structures optimized in Turbomole as input.

Experimental EPR measurements and spectral simulations:

Inspection of the EPR spectrum of **2** in a frozen 2-Me-THF solution clearly reveals besides the major species **2a** (~90% of the total spectral intensity), the presence of a second minor species **2b** (~5%), and a detailed line shape analysis suggests the presence of even a third minor species, **2c** (~5%) (Figure 3). The major species **2a** must correspond to [Ni(trop$_2$NH)(κ^2-OOCCF$_3$)], as the DFT calculated parameters of the optimized geometry of **2** correspond well to the experimental parameters of **1.**

The minor species **2b** and **2c** are perhaps 5-coordinate solvent adducts and/or species with a κ^1-OOCCF$_3$ coordination mode instead of the κ^2-OOCCF$_3$ coordination mode. The isotropic g-value (2.190) measured at 298 K (featureless, relatively broad isotropic signal) corresponds roughly with the weighted averaged anisotropic g-values of the species **2a**, **2b** and **2c**, suggesting that the rapidly frozen solution spectrum reflects approximately the kinetically trapped equilibrium distribution of these same species in solution. Although interesting, we did not investigate this aspect any further.

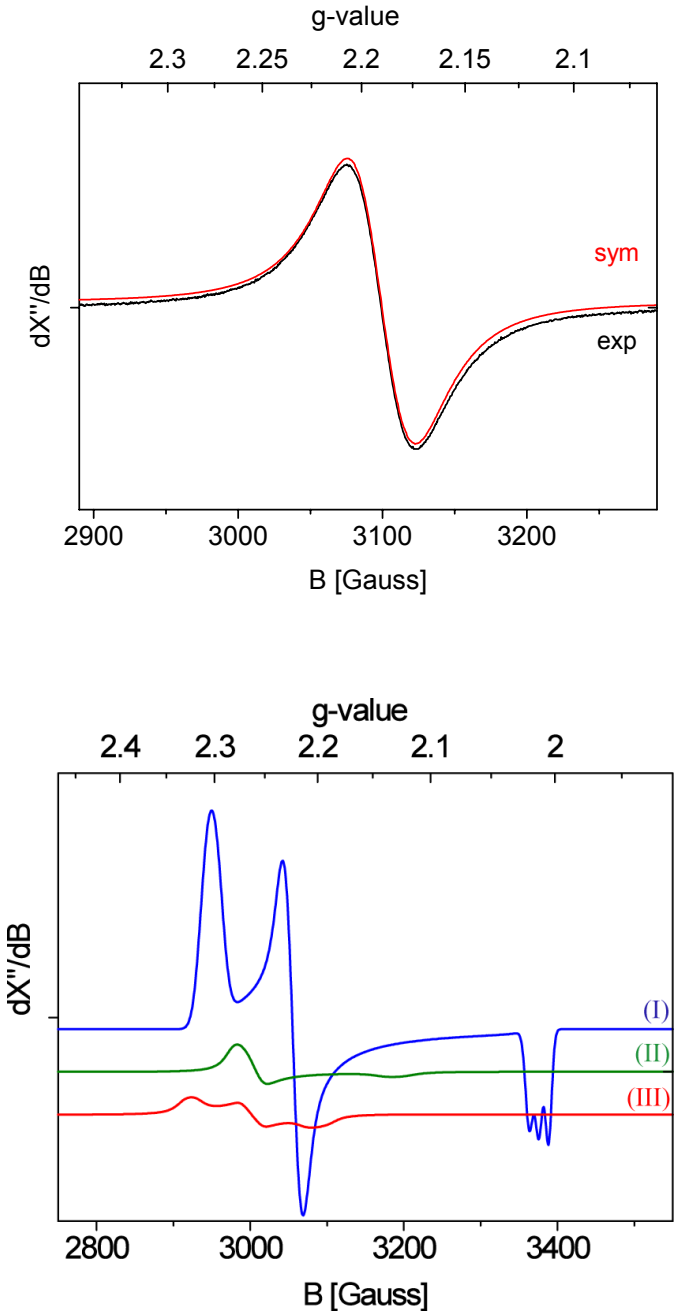

Figure 3.
Top: Experimental and simulated isotropic X-band EPR spectrum of [Ni(trop$_2$NH)(OOCCF$_3$)] **2** in 2-Me THF at 298 K. Experimental conditions: microwave frequency 9.500431 GHz, microwave power 0.401 mW, modulation amplitude 1.00 Gauss. *Bottom:* Individual components 2a (90%), 2b (4%) and 2c (6%) contributing to the EPR spectrum shown in the main text. The simulations were obtained using the parameters in Table 3.

Table 3. Experimental[(a)] and *DFT calculated*[(b)] EPR parameters.

	[Ni(trop$_2$NH)(OOCCF$_3$)] **2** *(a) (c)*	[Ni(trop$_2$NH)(OOCCF$_3$)] **2** *(b)*
g_x	2.303	*2.225 (2.196)*
g_y	2.223	*2.169 (2.128)*
g_z	2.012	*2.028 (1.998)*
g_{iso}	*2.190*	*2.141 (2.107)*
A_x^N	n.r.	*19 (20)*
A_y^N	n.r.	*19 (20)*
A_z^N	35	*30 (37)*
A_{iso}^N	n.r. (<30)	*22 (26)*
$\eta^{N\,(d)}$	-	*10%*
A_x^P	-	-
A_y^P	-	-
A_z^P	-	-
A_{iso}^P	-	-
$\eta^{P\,(d)}$	-	-
$\eta^{Ni\,(d)}$	-	*82%*

(a) Spectral simulation; Hyperfine couplings in MHz; n.r. = not resolved. Anisotropic spectra measured in frozen 2-Methyl THF at 120K. Isotropic spectra (g_{iso}, A_{iso}) measured at 298 K in 2-Methyl THF.
(b) Orca, PBE0/TZVP (ADF, BP86/TZP).
(c) Data for the major species. Line shape analysis suggests the presence of two additional minor species (~10% of the total intensity), each revealing rhombic g-tensors (2.278, 2.258, 2.130; ~ 4% and 2.324, 2.262, 2.200; ~6%) without resolved hyperfine couplings.
(d) η = Mulliken spin density population.

The experimental and DFT calculated EPR parameters of [Ni(trop$_2$NH)(κ^2-OOCCF$_3$)] **2** are comparable. The N-hyperfine couplings for [Ni(trop$_2$NH)(κ^2-OOCCF$_3$)] **2** are only resolved along g_z.

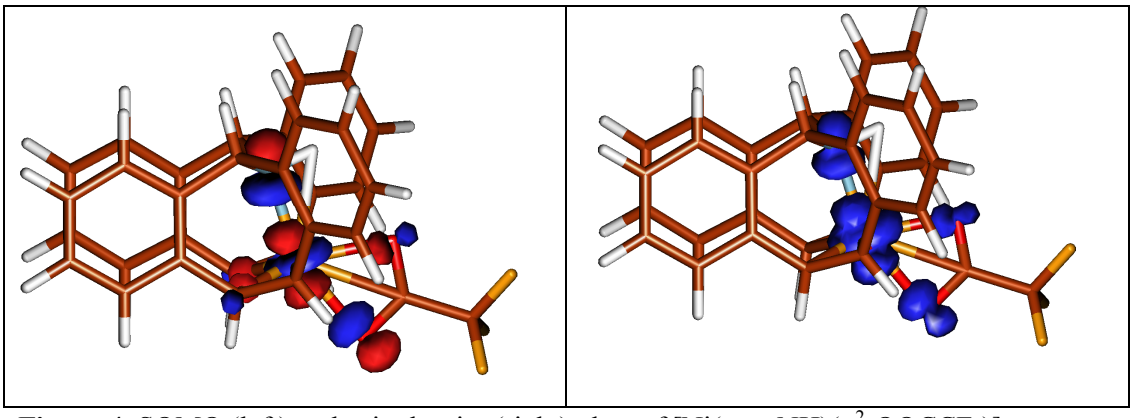

Figure 4. SOMO (left) and spin density (right) plots of [Ni(trop$_2$NH)(κ^2-OOCCF$_3$)]

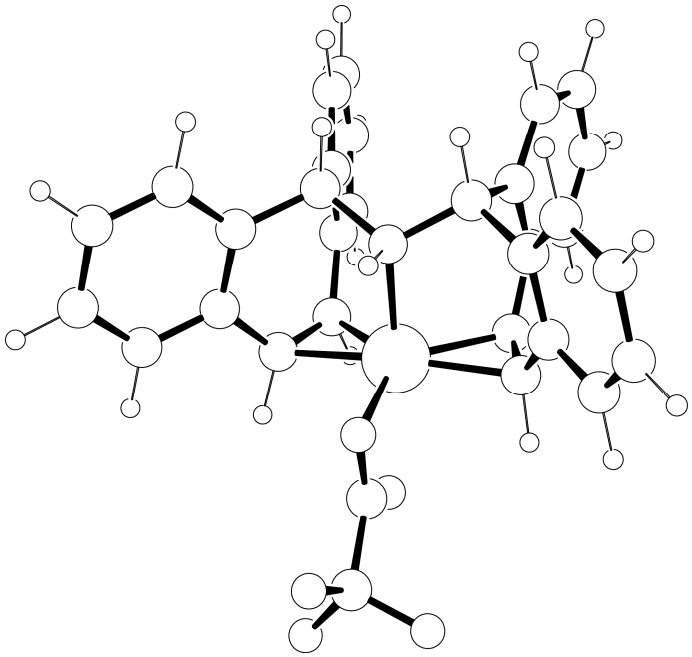

Figure 5. DFT optimized structure of [Ni(trop$_2$NH)(κ^2-OOCCF$_3$)] **2** (above) and list of atom coordinates (below).

ATOM	1	Ni	111	1	7.604	9.924	13.802	1.00 0.00
ATOM	2	O	111	1	8.838	9.028	12.192	1.00 0.00
ATOM	3	O	111	1	8.588	11.231	12.441	1.00 0.00
ATOM	4	C	111	1	9.281	9.816	15.024	1.00 0.00
ATOM	5	C	111	1	5.976	9.730	12.525	1.00 0.00
ATOM	6	F	111	1	11.010	9.669	10.570	1.00 0.00
ATOM	7	F	111	1	9.177	10.134	9.469	1.00 0.00
ATOM	8	F	111	1	10.308	11.731	10.444	1.00 0.00
ATOM	9	C	111	1	9.058	10.222	11.839	1.00 0.00
ATOM	10	C	111	1	9.910	10.451	10.566	1.00 0.00
ATOM	11	N	111	1	6.715	11.443	14.927	1.00 0.00
ATOM	12	C	111	1	4.842	8.986	14.701	1.00 0.00
ATOM	13	C	111	1	4.510	10.252	15.262	1.00 0.00
ATOM	14	C	111	1	5.219	11.516	14.805	1.00 0.00
ATOM	15	C	111	1	4.147	13.039	13.080	1.00 0.00
ATOM	16	C	111	1	7.026	10.310	17.165	1.00 0.00
ATOM	17	C	111	1	3.491	10.336	16.230	1.00 0.00
ATOM	18	C	111	1	6.365	10.400	18.405	1.00 0.00
ATOM	19	C	111	1	5.270	11.002	12.308	1.00 0.00
ATOM	20	C	111	1	4.175	7.837	15.196	1.00 0.00
ATOM	21	C	111	1	7.234	11.565	16.332	1.00 0.00
ATOM	22	C	111	1	4.856	11.857	13.369	1.00 0.00
ATOM	23	C	111	1	5.809	8.828	13.606	1.00 0.00
ATOM	24	C	111	1	8.702	11.953	16.285	1.00 0.00
ATOM	25	C	111	1	8.317	8.892	15.499	1.00 0.00

```
ATOM     26  C   111     1       9.639  11.114  15.618  1.00  0.00
ATOM     27  C   111     1       7.521   9.051  16.724  1.00  0.00
ATOM     28  C   111     1      11.399  12.763  16.097  1.00  0.00
ATOM     29  C   111     1       9.133  13.162  16.864  1.00  0.00
ATOM     30  C   111     1       6.154   9.267  19.204  1.00  0.00
ATOM     31  C   111     1       7.265   7.910  17.525  1.00  0.00
ATOM     32  C   111     1      10.474  13.569  16.782  1.00  0.00
ATOM     33  C   111     1       6.598   8.012  18.751  1.00  0.00
ATOM     34  C   111     1       3.170   7.934  16.165  1.00  0.00
ATOM     35  C   111     1      10.982  11.557  15.519  1.00  0.00
ATOM     36  C   111     1       3.854  13.404  11.756  1.00  0.00
ATOM     37  C   111     1       4.992  11.404  10.978  1.00  0.00
ATOM     38  C   111     1       4.288  12.583  10.701  1.00  0.00
ATOM     39  C   111     1       2.814   9.194  16.679  1.00  0.00
ATOM     40  H   111     1       4.863  12.351  15.453  1.00  0.00
ATOM     41  H   111     1       6.678  12.393  16.831  1.00  0.00
ATOM     42  H   111     1      10.058   9.390  14.365  1.00  0.00
ATOM     43  H   111     1       4.442   6.851  14.780  1.00  0.00
ATOM     44  H   111     1       7.630   6.929  17.179  1.00  0.00
ATOM     45  H   111     1       5.332  10.761  10.149  1.00  0.00
ATOM     46  H   111     1       5.993  11.383  18.744  1.00  0.00
ATOM     47  H   111     1       6.412   9.293  11.610  1.00  0.00
ATOM     48  H   111     1       5.629   9.360  20.169  1.00  0.00
ATOM     49  H   111     1       8.397  13.804  17.379  1.00  0.00
ATOM     50  H   111     1       6.120   7.786  13.408  1.00  0.00
ATOM     51  H   111     1      11.710  10.925  14.985  1.00  0.00
ATOM     52  H   111     1       6.428   7.109  19.360  1.00  0.00
ATOM     53  H   111     1       3.235  11.323  16.652  1.00  0.00
ATOM     54  H   111     1       8.458   7.847  15.169  1.00  0.00
ATOM     55  H   111     1       7.094  12.249  14.400  1.00  0.00
ATOM     56  H   111     1       3.832  13.693  13.911  1.00  0.00
ATOM     57  H   111     1       2.658   7.024  16.519  1.00  0.00
ATOM     58  H   111     1       2.023   9.284  17.441  1.00  0.00
ATOM     59  H   111     1       3.303  14.336  11.550  1.00  0.00
ATOM     60  H   111     1      10.791  14.522  17.236  1.00  0.00
ATOM     61  H   111     1      12.452  13.077  16.009  1.00  0.00
ATOM     62  H   111     1       4.080  12.864   9.656  1.00  0.00
CONECT    1    3    4    5   11   23   25
CONECT    2    9
CONECT    3    9
CONECT    4   25   26   42
CONECT    5   19   23   47
CONECT    6   10
CONECT    7   10
CONECT    8   10
CONECT    9   10
CONECT   11   14   21   55
CONECT   12   13   20   23
CONECT   13   14   17
CONECT   14   22   40
```

CONECT 15 22 36 56
CONECT 16 18 21 27
CONECT 17 39 53
CONECT 18 30 46
CONECT 19 22 37
CONECT 20 34 43
CONECT 21 24 41
CONECT 23 50
CONECT 24 26 29
CONECT 25 27 54
CONECT 26 35
CONECT 27 31
CONECT 28 32 35 61
CONECT 29 32 49
CONECT 30 33 48
CONECT 31 33 44
CONECT 32 60
CONECT 33 52
CONECT 34 39 57
CONECT 35 51
CONECT 36 38 59
CONECT 37 38 45
CONECT 38 62
CONECT 39 58
END

H. References

[1] R. K. Harris, E. D. Becker, S. M. C. de Menezes, R. Goodfellow, P. Granger, *Pure and Applied Chemistry* **2001**, *73*, 1795.

[2] T. Büttner, F. Breher, H. Grützmacher, *Chem. Commun.* **2004**, 2820.

[3] K[Me_2NBH_3] **5** was prepared by treatment of Me_2HN-BH_3 **4** with 1.0 equiv of KH in THF at room temperature, according to the method adapted from: R. O. Hutchins, K. Learn, F. El-Telbany, Y. P. Stercho, *J. Org. Chem.* **1984**, 49, 2438.

[4] C. A. Jaska, K. Temple, A. J. Lough, I. Manners *Chem. Commun*. **2001**, 962.

[5] H. Noeth, S. Thomas, *Eur. J. Inorg. Chem.* **1999**, 1373.

[6] a) R. Ahlrichs, M. Bär, H.-P. Baron, R. Bauernschmitt, S. Böcker, M. Ehrig, K. Eichkorn, S. Elliott, F. Furche, F. Haase, M. Häser, C. Hättig, H. Horn, C. Huber, U. Huniar, M. Kattannek, A. Köhn, C. Kölmel, M. Kollwitz, K. May, C. Ochsenfeld, H. Öhm, A. Schäfer, U. Schneider, O. Treutler, K. Tsereteli, B. Unterreiner, M. von

Arnim, F. Weigend, P. Weis, H. Weiss, *Turbomole Version 5*, January **2002**. Theoretical Chemistry Group, University of Karlsruhe; b) O. Treutler, R. Ahlrichs, *J. Chem. Phys.* **1995**, *102*, 346; c) Turbomole basisset library, Turbomole Version 5, see a); d) A. Schäfer, H. Horn, R. Ahlrichs, *J. Chem. Phys.* **1992**, *97*, 2571; e) D. Andrae, U. Haeussermann, M. Dolg, H. Stoll, H. Preuss, *Theor. Chim. Acta* **1990**, *77*, 123; f) A. Schäfer, C. Huber, R. Ahlrichs, *J. Chem. Phys.* **1994**, *100*, 5829.

[7] a) PQS version 2.4, **2001**, Parallel Quantum Solutions, Fayetteville, Arkansas, USA (the Baker optimizer is available separately from PQS upon request); b) J. Baker *J. Comput. Chem.* **1986**, *7*, 385.

[8] a) A. D. Becke *Phys. Rev. A* **1988**, *38*, 3098; b) J. P. Perdew *Phys. Rev. B* **1986**, *33*, 8822.

[9] Lead reference for calculation of g-tensor (Zeeman interactions) parameters: E. van Lenthe, A. van der Avoird, P. E. S Wormer, *J. Chem. Phys.* **1997**, *107*, 2488. Lead reference for calculation of A-tensor (Nuclear magnetic dipole hyperfine interactions) parameters: E. van Lenthe, A. van der Avoird, P. E. S. Wormer, *J. Chem. Phys.* **1998**, *108*, 4783.

[10] Neese, F. et al. *ORCA*, version 2.7, Revision 0, January **2010**; University of Bonn, Theoretical Chemistry.

[11] C. Adamo, V. Barone, *J. Chem. Phys.* **1999**, *110*, 6158.

[12] ADF2006 a) E.J. Baerends, D. E. Ellis, P. Ros, *Chem. Phys.* **1973**, *2*, 41. b) L. Versluis, T. Ziegler, *J. Chem. Phys.,* **1988**, *88*, 322. c) G. te Velde, E. J. Baerends, *J. Comput. Phys.*, **1992**, *99*, 84. d) C. Fonseca Guerra, J. G. Snijders, G. te Velde, E. J. Baerends, *Theor. Chem. Acc.,* **1998**, *99*, 391.

I. Analytical Data

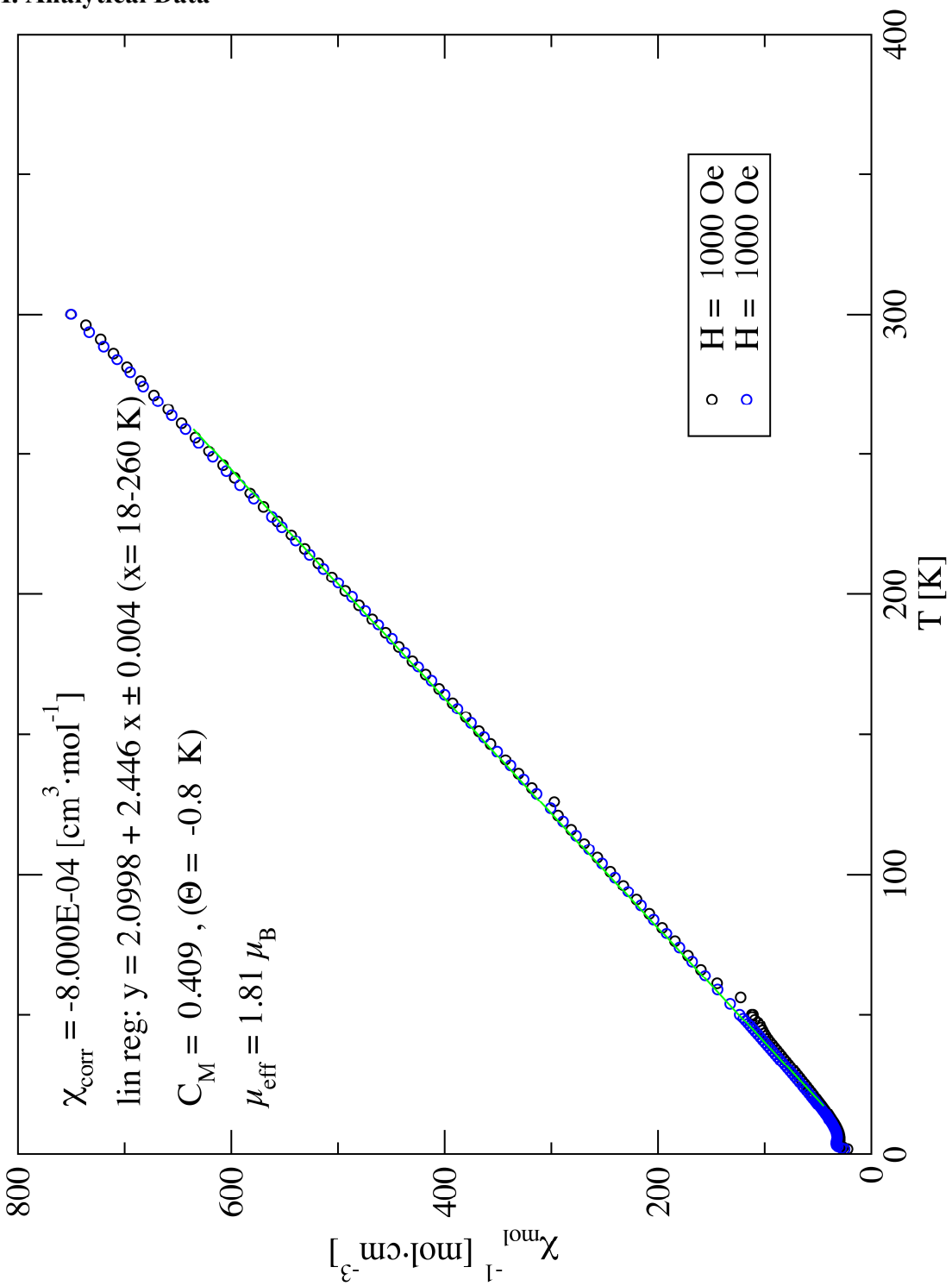

Figure 6. Resulting plot (χ_{mol} vs. T) of SQUID magnetic measurement of [Ni(trop$_2$NH)(OOCCF$_3$)] **2.**

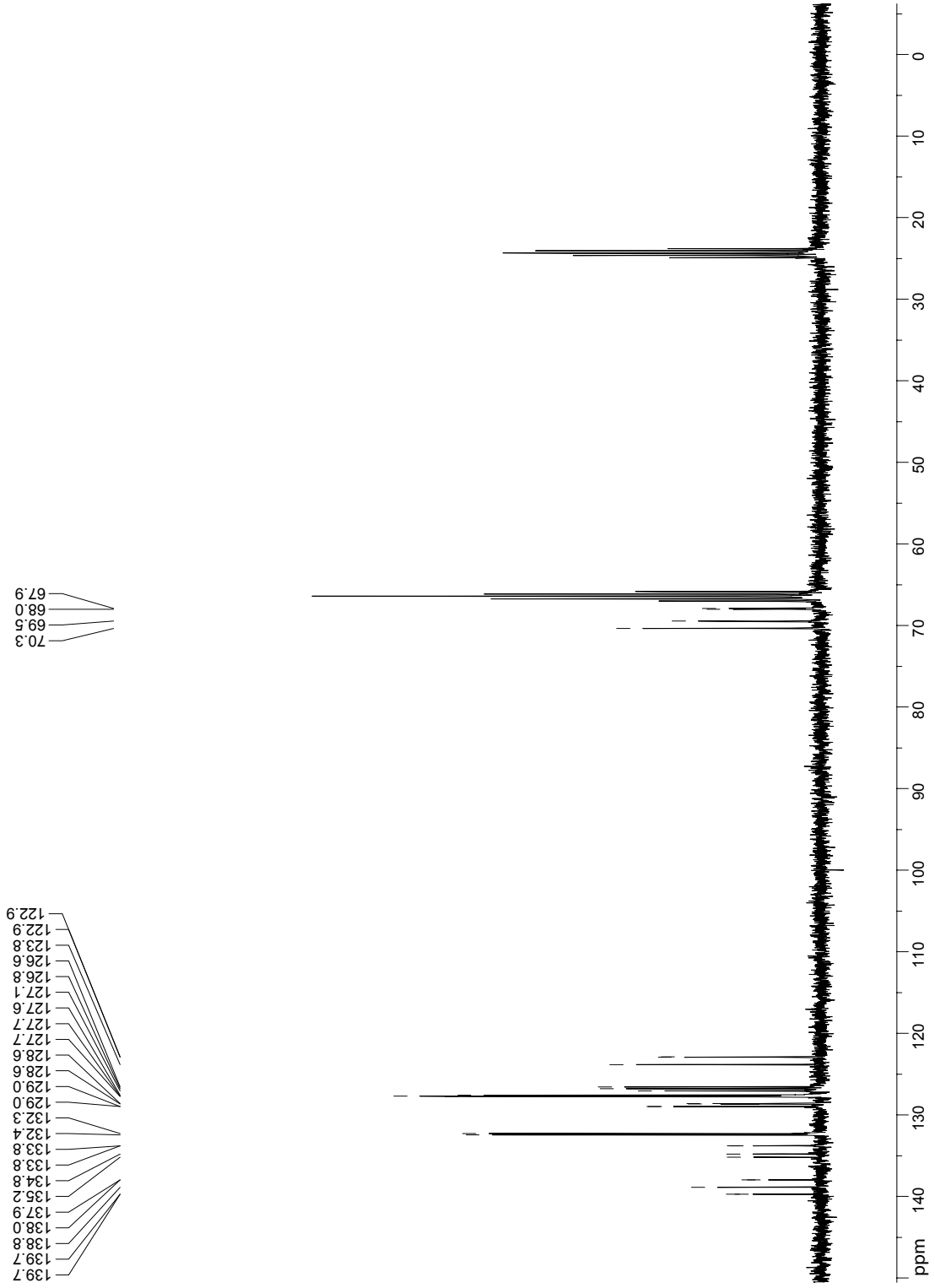

Figure 7. ^{13}C NMR spectrum [Ni($trop_2NH(PPh_3)$] **3** (75 MHz, [D_8]-THF).

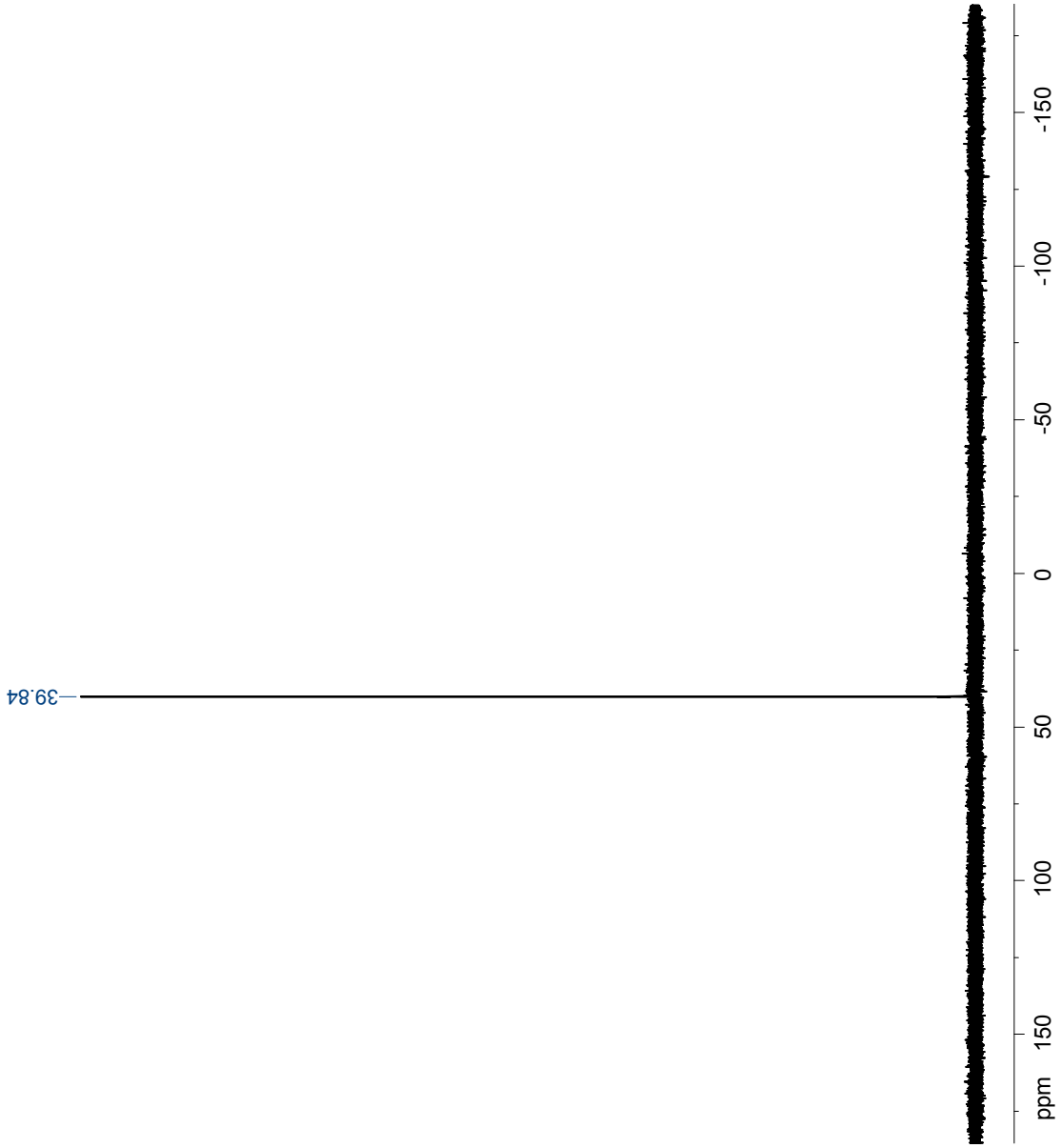

Figure 8. ^{31}P NMR spectrum [Ni($trop_2NH(PPh_3)$)] **3** (101.3 MHz, [D_8]-THF).

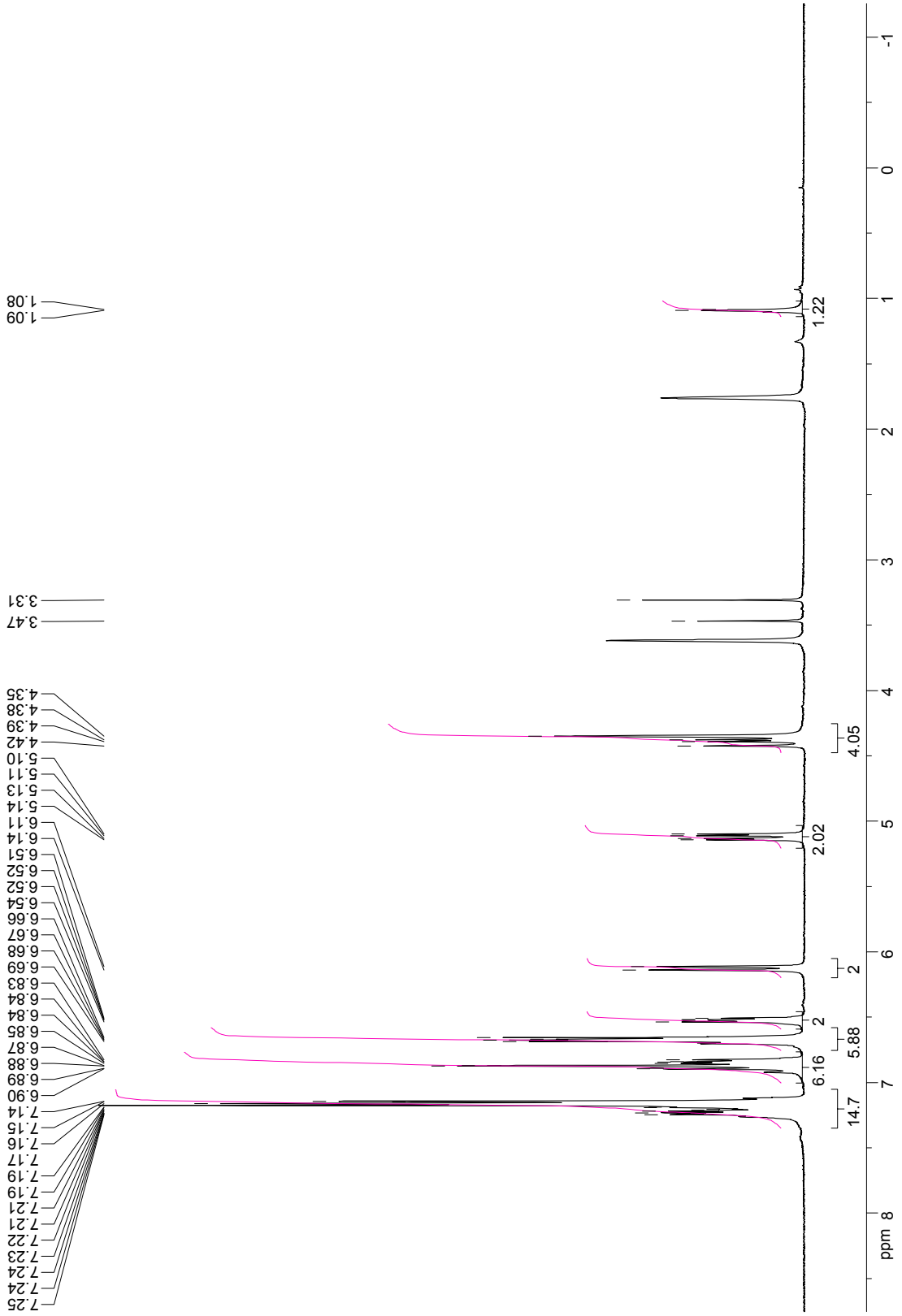

Figure 9. ^{1}H NMR spectrum [Ni(trop$_2$NH(PPh$_3$)] **3** (300 MHz, [D$_8$]-THF).

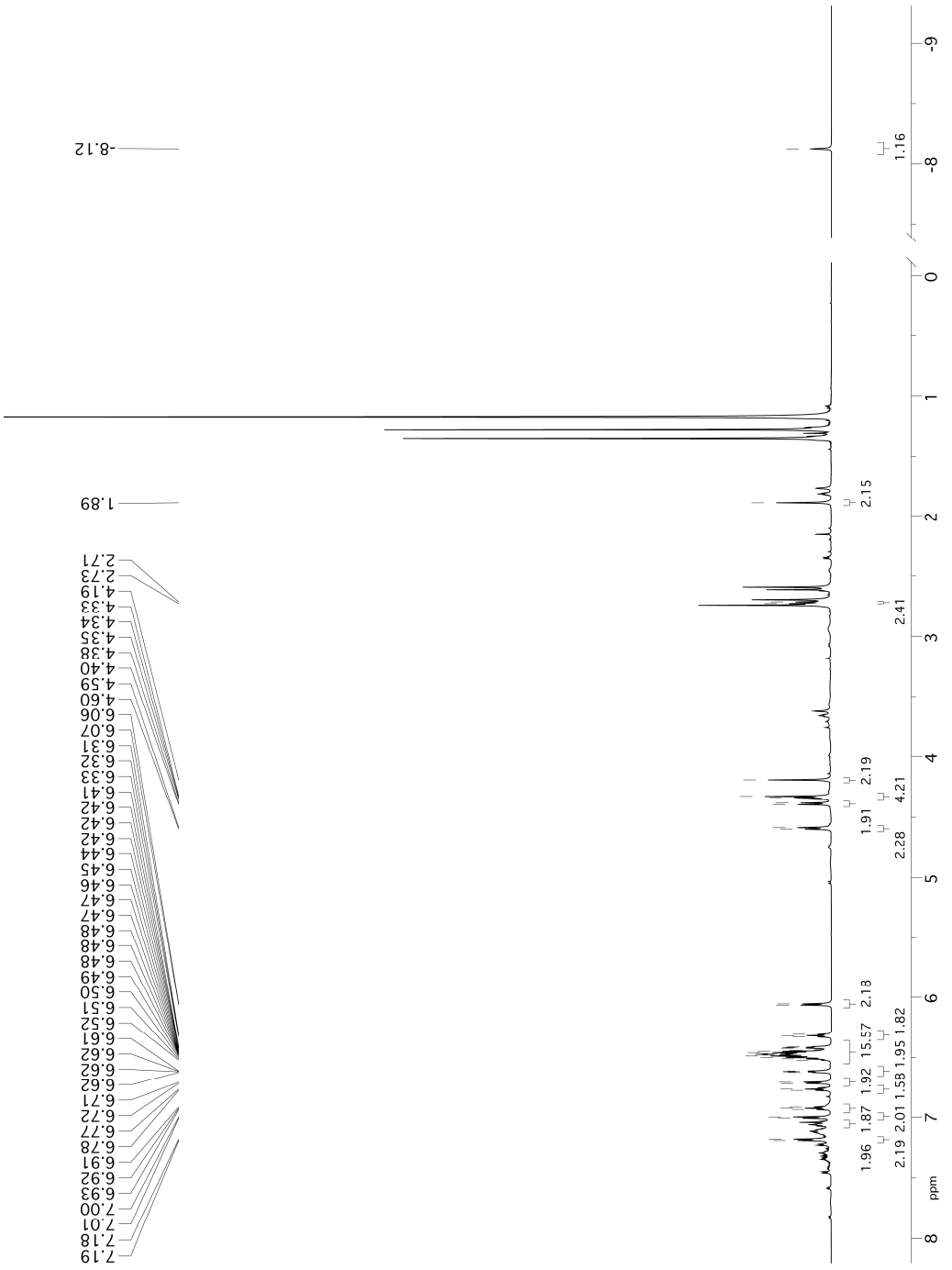

Figure 10. ^{1}H NMR spectrum of [K][(Ni(trop$_2$NH))$_2$(H)] **8** (700.13 MHz, [D$_8$]-THF)) in the reaction mixture according to experiment a) in Figure 1.

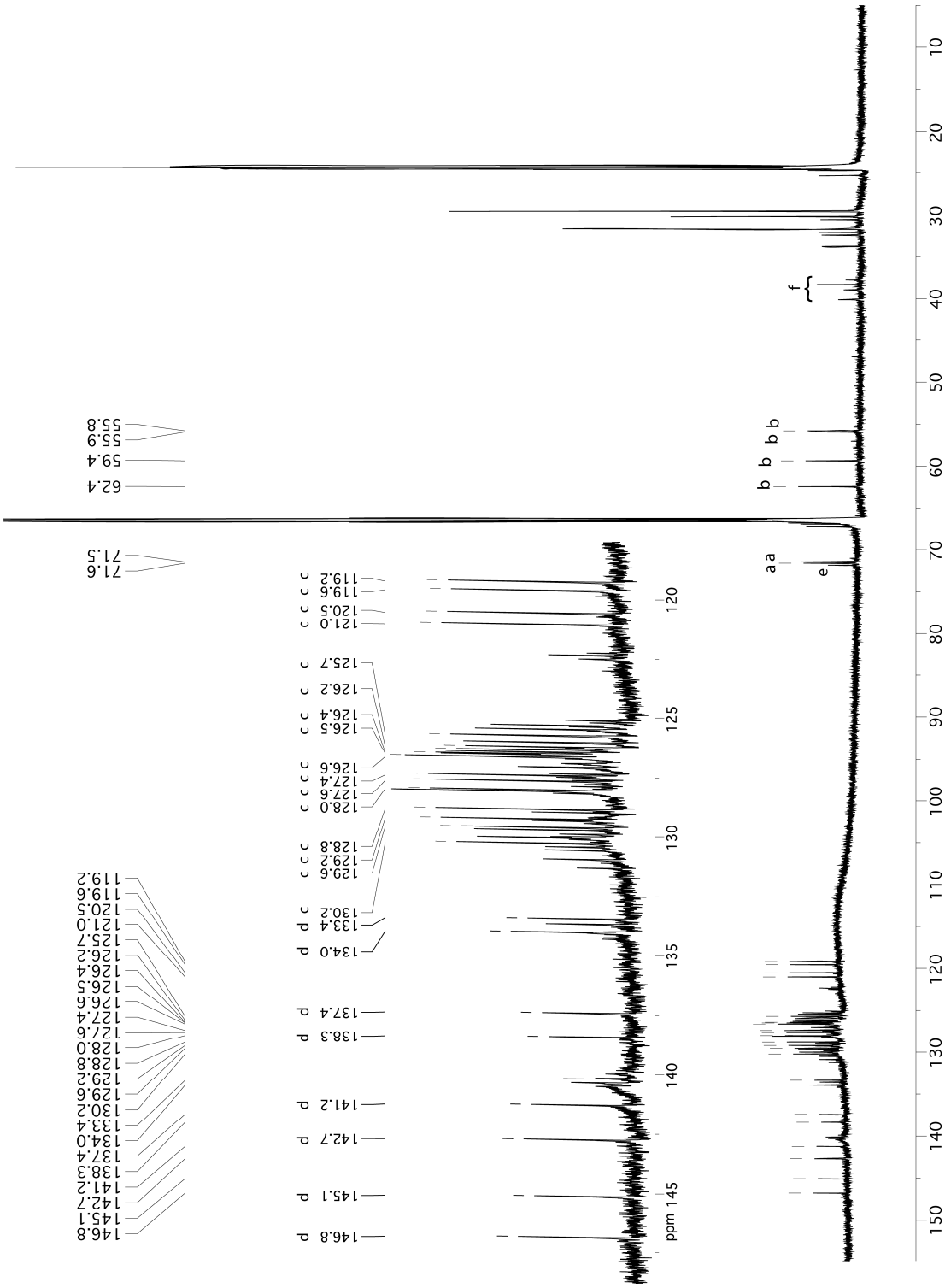

Figure 11. ^{13}C NMR spectrum of [K][(Ni(trop$_2$NH))$_2$(H)] **8** (176.1 MHz, [D$_8$]-THF) in the reaction mixture according to experiment a) in Figure 1. Numbering: a) C_{olefin}, b) C_{bzl}, c) CH_{aromat}, d) C_{quart}, e) C_{quart} (^{t}BuO), f) see Figure 12.

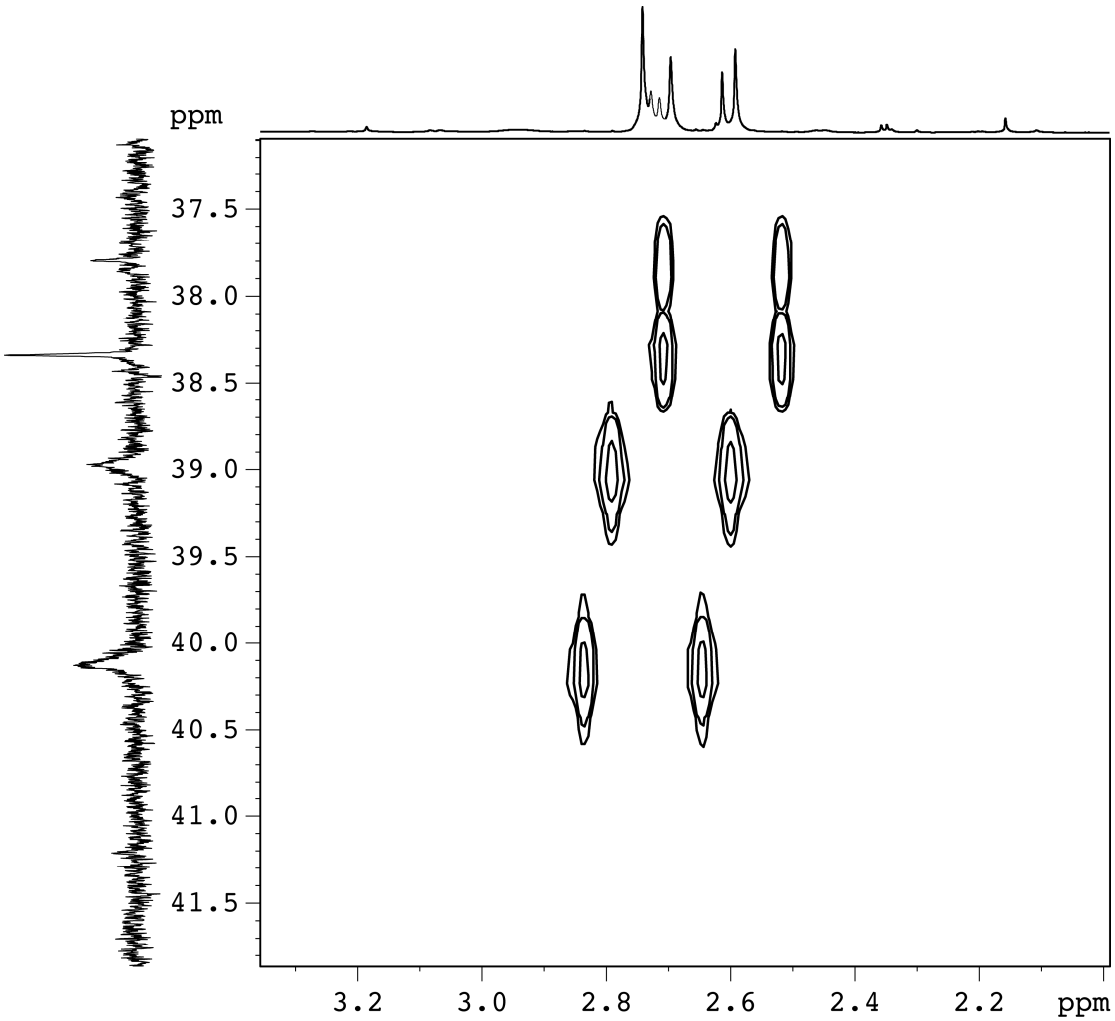

Figure 12. Section of the ^{1}H ^{13}C HMQC NMR spectrum (700.13 MHz, 298 K, [D8]-THF) of the reaction mixture according to experiment a) in Figure 1. The ^{1}H resonances 2.61–2.75 ppm show significant cross-peaks to the correlated ^{13}C NMR resonances at 38.3–40.3 ppm .The long-range correlation spectrum ^{1}H ^{13}C HMBC NMR spectrum (700.13 MHz, 298 K, [D8]-THF) shows no correlation to quarternary or *C*H aromatic ^{13}C resonances. In conclusion, both ^{1}H ^{13}C NMR correlation experiments give rise to exclude the ^{13}C signals between 38.8–40.3 ppm and ^{1}H resonances in range of 2.61–2.75 ppm from corresponding to partially hydrogenated trop-units.

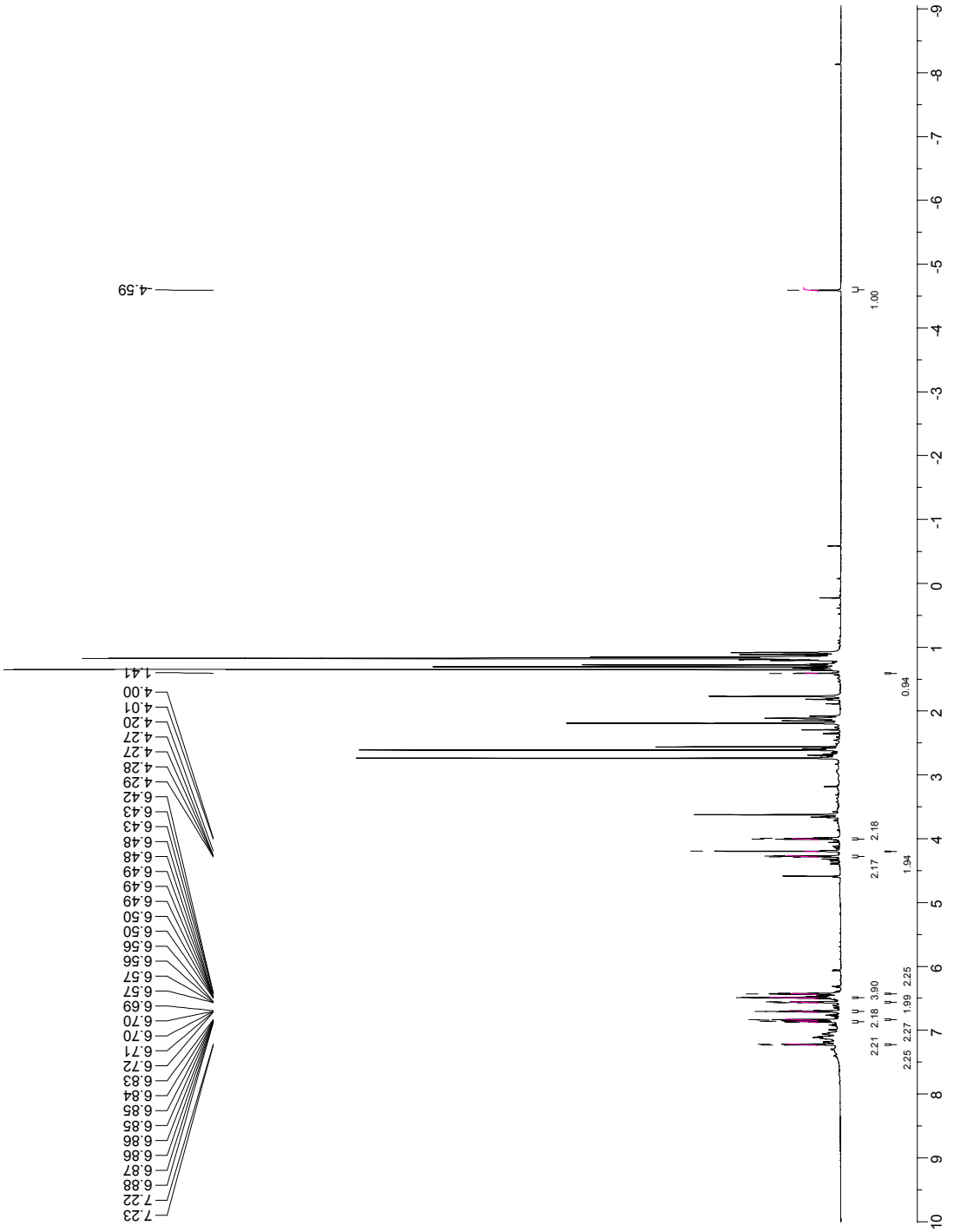

Figure 13. ^{1}H NMR spectrum of [K][Ni(trop$_2$NH)(H)] **9** (700.13 MHz, [D$_8$]-THF)) in the reaction mixture according to experiment c) in Figure 1.

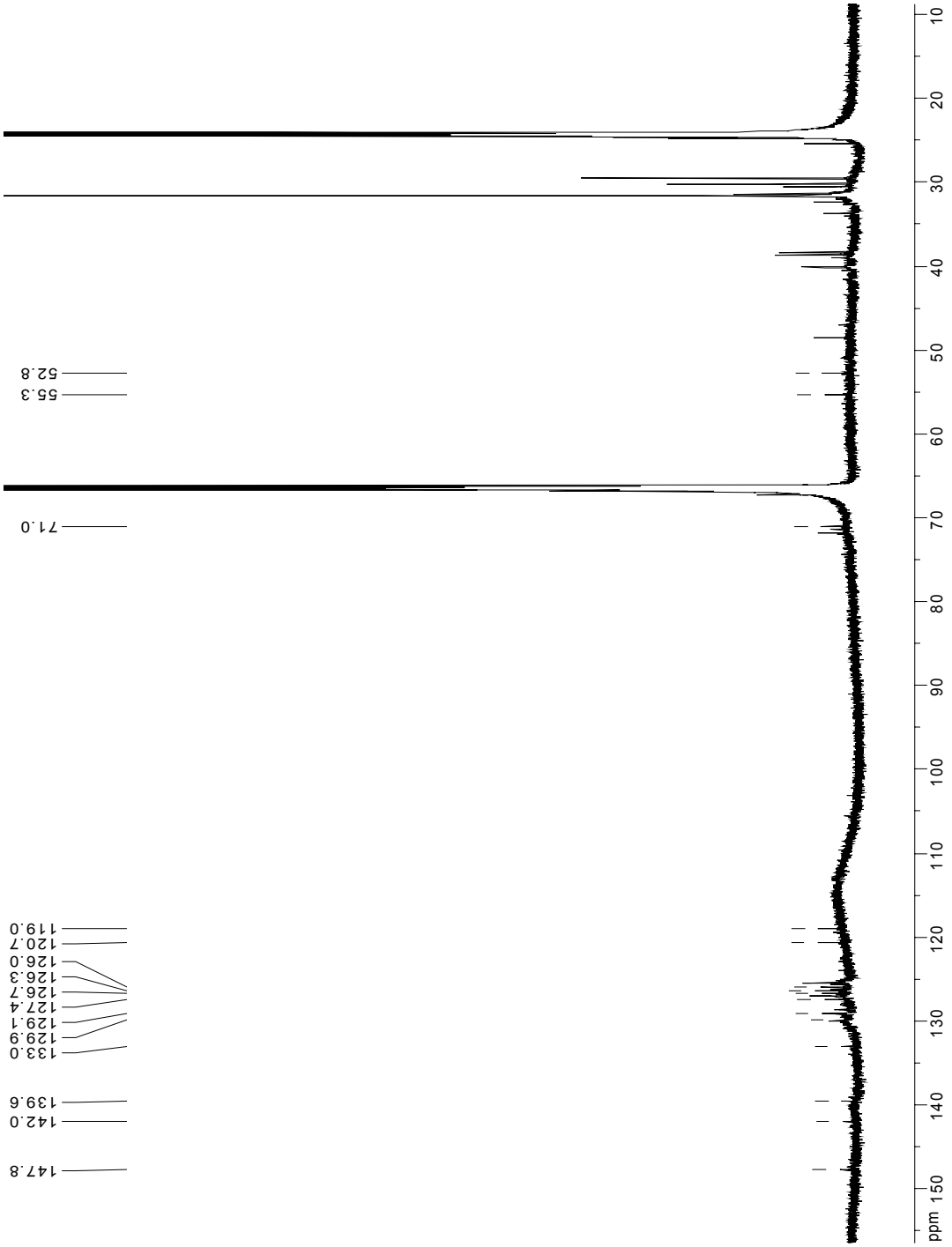

Figure 14. ^{13}C NMR spectrum of [K][Ni(trop$_2$NH)(H)] **9** (176.1 MHz, [D$_8$]-THF)) in the reaction mixture according to experiment c) in Figure 1.

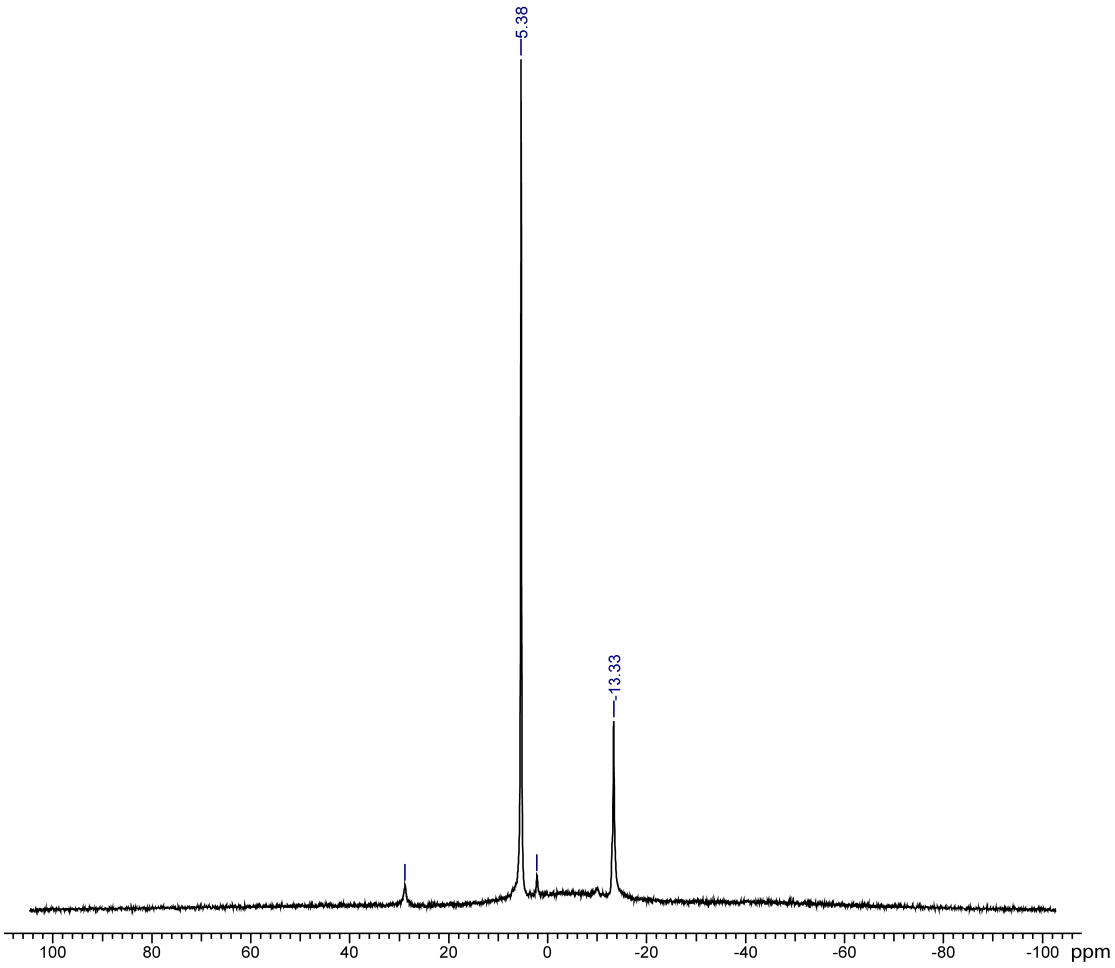

Figure 15 : $^{11}B\{^{1}H\}$NMR spectrum (96.3 MHz, [D_8]-THF) of the *in situ* performed stoichiometric reaction (ii) of '**Scheme 3.** Different reaction pathways of [$Ni^{I}(trop_2NH)(OOCCF_3)$] **2** to Ni^{0} complexes **3**, **8**, and **9** in the presence of amine borane **4** and amido borane **5**.
Traces of compound **7** are observed at 1.8 ppm (BH_2) and the corresponding resonance of BH_3 is overlapped by the signal of Me_2HN-BH_3. Traces of $BH(NMe_2)_2$ at 28.4 and $Me_2N{=}BH_2$ at 37.4 ppm are also observed

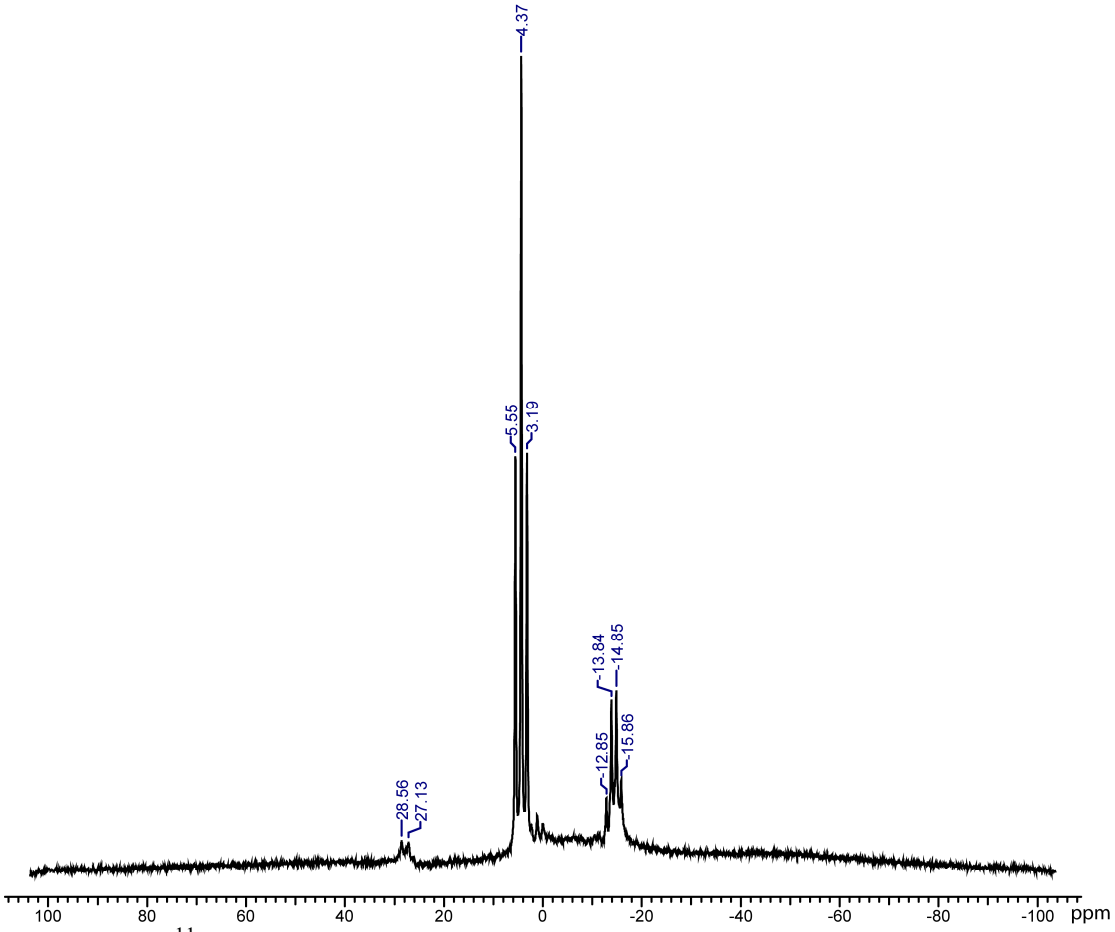

Figure 16 : ^{11}B NMR spectrum (96.3 MHz, [D_8]-THF) of the *in situ* performed stoichiometric reaction (ii) of '**Scheme 3.** Different reaction pathways of [Ni^{I}(trop$_2$NH)(OOCCF$_3$)] **2** to Ni^{0} complexes **3**, **8**, and **9** in the presence of amine borane **4** and amido borane **5'**.
Traces of BH(NMe$_2$)$_2$ at 28.4 ppm ($^{1}J_{BH}$ = 137 Hz) are observed.

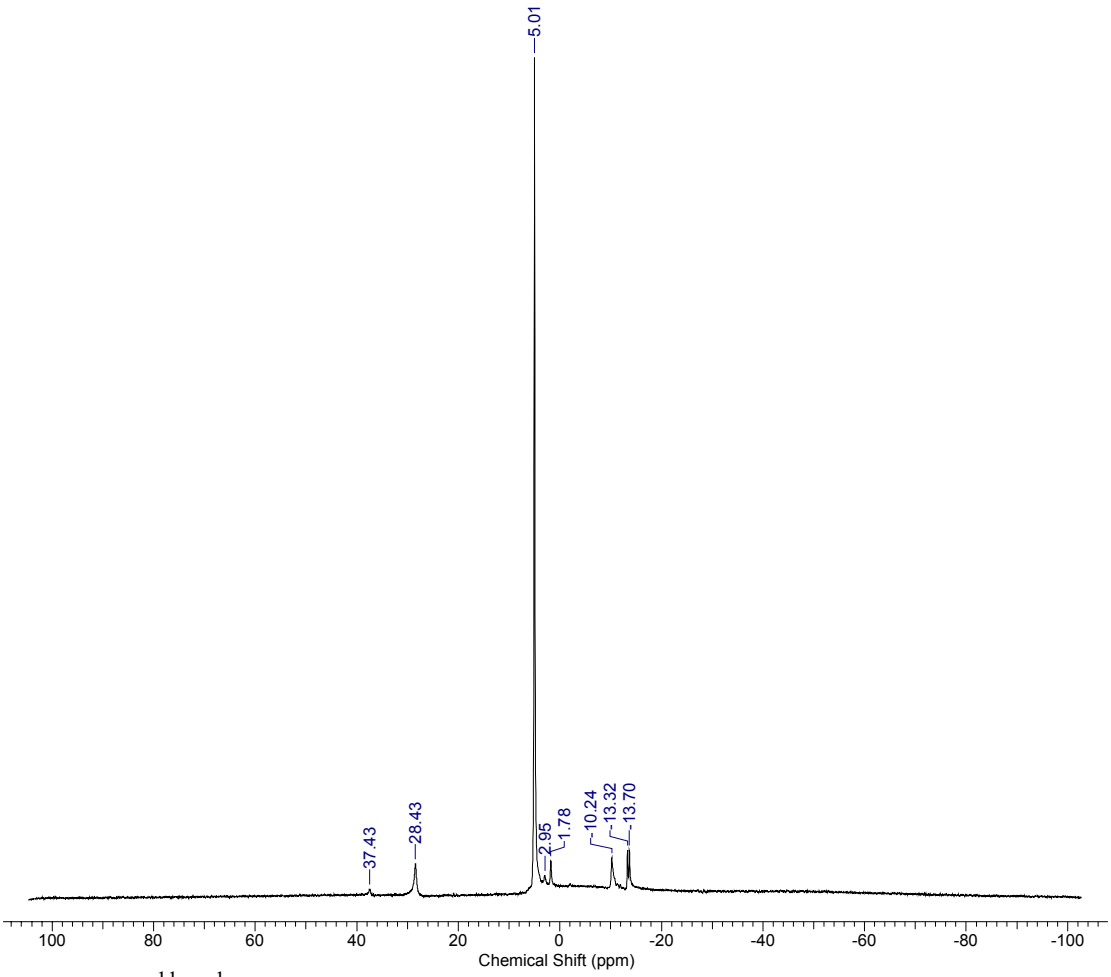

Figure 17. $^{11}B\{^{1}H\}$NMR spectrum (96.3 MHz, [D_8]-THF) of the *in situ* performed stoichiometric reaction (iii) of '**Scheme 3.** Different reaction pathways of [Ni^{I}(trop$_2$NH)(OOCCF$_3$)] **2** to Ni^{0} complexes **3**, **8**, and **9** in the presence of amine borane **4** and amido borane **5'**.

Traces of compound **7** are observed at 1.8 ppm (BH_2) and the corresponding resonance of BH_3 is overlapped by the signal of Me_2HN-BH_3. Traces of $BH(NMe_2)_2$ at 28.4 and $Me_2N{=}BH_2$ at 37.4 ppm are also observed.

Cyclic Voltammograms of Complex 2 and 3

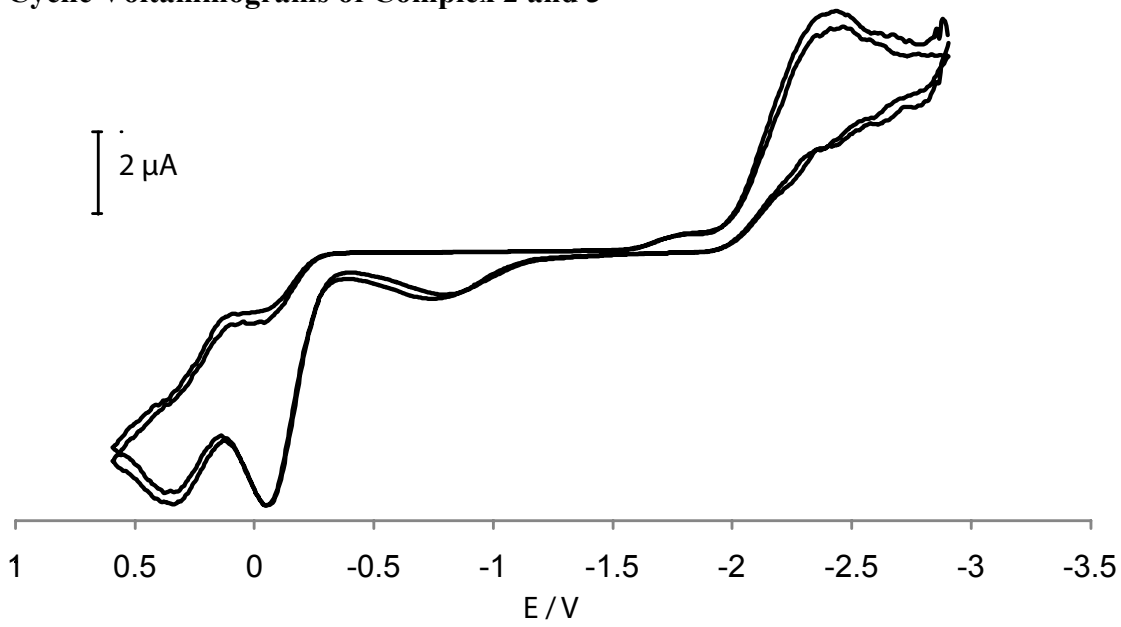

Figure 17. Cyclic voltamogramm of [Ni(trop$_2$NH(OOCCF$_3$)] **2**, at 253 K, in THF, 1 M TBAPF$_6$ (TBA = tetra butyl ammonium) as supporting electrolyte, scan rate 100 mV/s, referenced to Fc/Fc$^+$. On-set potential -1.99 V; peak potential -2.42 V.

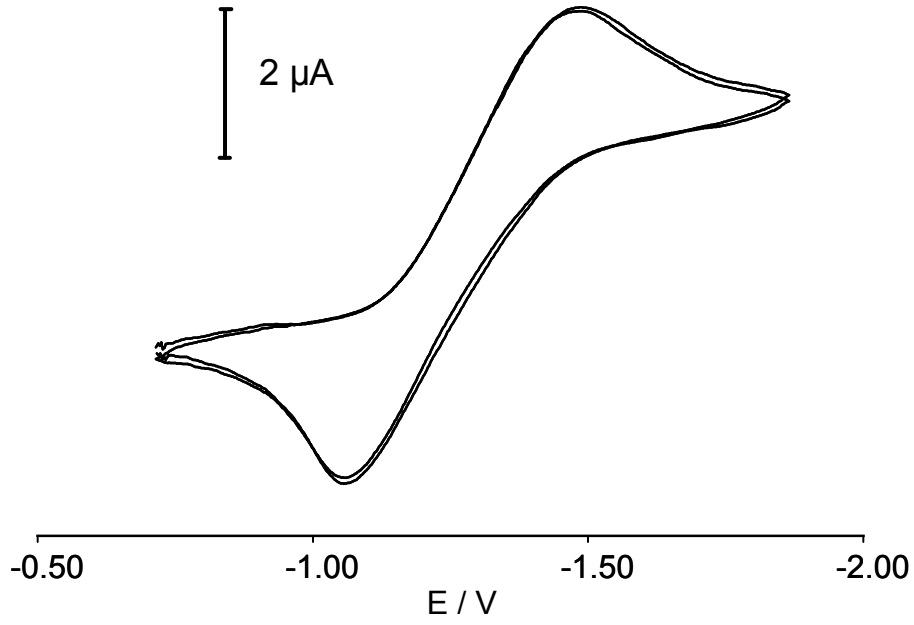

Figure 18. Cyclic voltammogram of [Ni(trop$_2$NH(PPh$_3$)] **3**, at 298 K, in THF, 1 M TBAPF$_6$ as supporting electrolyte, scan rate 100 mV/s, referenced to Fc/Fc$^+$ $E_{1/2}$ = -1.28 V.